# Exciton spectra and polarization fields modified by quantum-dot confinements

Jia-Lin Zhu,* Ning Yang, and Baolei Li
*Department of Physics, Tsinghua University, Beijing 100084, China*

Weidong Chu and Zhensheng Dai
*Institute of Applied Physics and Computational Mathematics, P.O. Box 8009(28), Beijing 100088, China*
(Received 18 March 2009; revised manuscript received 17 July 2009; published 12 August 2009)

We have investigated exciton states and their energy spectra in GaN/$Al_xGa_{1-x}N$ quantum dots with different confinement strengths using a variational-diagonalization method. Under a weak confinement, the transition of exciton states from completely to incompletely confined cases is shown, as the dot size becomes less than the critical size and only one kind of carrier can be well confined in the dot. Evolutions of binding energy and energy spectra with dot size are studied and different quantum behaviors of incompletely confined excitons are revealed. The oscillator strengths and the full width at half maximum of polarization fields are also calculated and their abnormal increases in the incomplete confinement regime are predicted.

DOI: 10.1103/PhysRevB.80.075306 PACS number(s): 78.66.Fd, 78.67.Hc, 73.21.−b

## I. INTRODUCTION

Semiconductor quantum dots (QDs) have great application potentials in future quantum-optical and quantum-information devices due to their excellent optical properties, such as narrow optical linewidths, stable photon flux, and so on. Quantum-confined excitons dominate the optical emission and absorption of QDs.[1–3] The unique optical property of semiconductor QDs can be attributed to quantum confinement of carriers, which leads to quantumlization of their energy levels and enhancement of optical transition.[4,5] The optical properties of QDs strongly depend on the shape[6] and size of the confinement potential. Generally, the smaller the dot size is, the stronger the confinement of their carriers is, and hence, the better its optical performance is. In experiment, to make full use of the advantage of QDs people usually fabricate QDs with their size approaching or less than the exciton Bohr radius in bulk material $a_B^*=\epsilon\hbar^2/\mu e^2$, where $\mu$ is the reduced mass of exciton, $\epsilon=4\pi\varepsilon_0\varepsilon_r$ with $\varepsilon_0$ the vacuum permittivity, and $\varepsilon_r$ the static dielectric constant. $a_B^*$ serves as a characteristic length scale for dot size that we can achieve in fabricating.

Unlike quantum well, however, there is not always a bound state for a carrier in the finite three-dimensional confining potential provided by a QD. There is a critical size to confine a carrier. Take a spherical QD with square potential as an example, the critical radius is $R_{ci}=(\hbar\pi)/(\sqrt{8m_i^*V_i})$, where $m_i^*$ and $V_i$ are effective mass and barrier height, $i=e(h)$ means electron (hole). The smaller (lower) the effective mass is (barrier height), the bigger the critical size is. Assuming that the critical size for electrons is bigger than that for holes, if dot size is smaller than both critical sizes, then the exciton cannot be confined. While in QDs with their sizes in the incomplete confinement regime, that is, between critical size for electron and that for hole, the electron by itself cannot be confined. Owing to the attractive Coulomb interaction, however, the electron can still be localized by the confined hole and the exciton as a whole is confined. This is so-called incompletely confined exciton.[7] Correspondingly, we call excitons confined in QDs with their sizes bigger than both critical sizes completely confined excitons.

For conventional GaAs/AlGaAs quantum dots, band offsets are large enough and both carriers can be well confined, since $R_{ce}$ (about 2.3 nm) is much less than $a_B^*$ (about 12 nm).[8] Nevertheless, in GaN/$Al_xGa_{1-x}N$ QDs with small $x$, $R_{ce}$ (about 2 nm) is very close to the corresponding $a_B^*$ (about 3 nm).[9,10] In fact, the sizes of QDs prepared in some experiments have approached this critical size.[11] And for self-assembled QDs fabricated through Stranski-Krastanov mode, the dot size and its distribution depend strongly on the growth condition,[10] and hence the incompletely confined exciton states can be introduced and novel photoelectric properties may be discovered.

Recently GaN related III-V semiconductor QDs draw great interest owing to their scientific values and promising applications for optoelectronic devices.[10,12] A large number of works have been reported on fabrication and characterization,[13] optical properties[10,11,14,15] and the effect of built-in electric field1.[1,14–16] And it has been proposed to control the oscillator strength of an exciton by external field.[2] Yet, the incompletely confined effect has not been given sufficient attention. In present work, we attempt to investigate exciton states in quantum dots with different confinement strengths to reveal the different characteristics between completely and incompletely confined excitons, and better understand the reason behind them.

To find a set of proper basis and solve the model Hamiltonian with good convergence, we adopt a variation-diagonalization (VD) method within the framework of effective-mass approximation.[17] By calculating critical curves for carriers having bound states, the incomplete confinement regime is determined. Distinct-quantum properties of incompletely confined excitons are revealed through investigating the binding energies, energy spectra, oscillator strengths, and polarization-field distributions in QDs with different sizes. The rest of this paper is organized as follows: in Sec. II, we introduce the model exciton Hamiltonian and the VD method. Section III is devoted to calculated results and discussions, followed by a brief conclusion in Sec. IV.

 

## II. MODEL AND METHOD

### A. Hamiltonian

Because of low barrier and small dot size, the numerical solution of incompletely confined excitons is much more difficult than that of general ones. Finite model potentials, instead of the usually used infinite ones, must be adopted. For an exciton confined in a disklike QD, the model Hamiltonian can be written as

$$\hat{H}_{ex} = \sum_{i=e,h} \left\{ \frac{\hat{p}_i^2}{2m_i^*} + U_i \right\} - \frac{e^2}{\epsilon |\vec{r}_e - \vec{r}_h|}, \tag{1}$$

where $U_i$ is the finite confinement potential. It can be described by

$$U_i(\vec{r}_i) = \begin{cases} V_i^0, & \text{if } |z_i| \geq \dfrac{H}{2} \\ V_i^0 f(\vec{\rho}_i), & \text{if } |z_i| < \dfrac{H}{2} \end{cases}, \tag{2}$$

where $\vec{r}_i$ are three-dimensional cylindrical coordinates $\vec{r}_i = (\vec{\rho}_i, z_i)$, $V_i^0$ is the discontinuity of conductance band ($e$) or valance band ($h$). The function $f(\vec{\rho}_i)$ corresponds to the lateral confinement of QDs, which can simulate a finite parabolic lateral confinement with

$$f(\vec{\rho}_i) = \begin{cases} \dfrac{\rho_i^2}{R^2}, & \text{if } |\rho_i| < R \\ 1, & \text{if } |\rho_i| \geq R \end{cases} \tag{3}$$

or a finite square-lateral confinement with

$$f(\vec{\rho}_i) = \begin{cases} 0, & \text{if } |\rho_i| < R \\ 1, & \text{if } |\rho_i| \geq R \end{cases}. \tag{4}$$

Several points should be mentioned here for our model. First, in our calculation, the built-in field is neglected to emphasize the effects of incomplete confinement. This is based on the following considerations. First, although built-in electric field in wurtzite GaN/AlN is strong, it is relatively weak in $GaN/Al_xGa_{1-x}N$ QDs with small $x$.[18] Second, the incomplete confinement effect occurs in very small QDs where the potential effect of built-in electric field is depressed, the behaviors of the electron and the hole are governed mainly by quantum confinement. Third, built-in electric field is usually applied along the growth direction while in lateral plane it is not so significant and only brings little modification to the two-dimensional confinement potential.[18,19] Our discussion about exciton states is focused on lateral motion and the exact shape of confinement potential has only small effect on properties of incompletely confined excitons as indicated by our calculations.

The second point is that we neglect the variation in static dielectric constant $\varepsilon_r$ as the dot size changes. Although some works suggest that it varies with dot size, this variation is not significant unless the dot size is too small (with diameter less than 0.6 nm).[20] Also neglected is the slight difference (note that $x$ is small) of material parameters in and out the dot. After all, inclusion of these factors only brings little quantitative difference and our assumption does not diminish the validity of our calculation.

### B. VD method

Due to entanglement of $z$ part and lateral in-plane part, even a direct numerical solution to the single-particle eigenstates without Coulomb interaction under the confinement potential $U_i$ described in Eq. (2) is difficult. To address this problem, we adopt the VD method[17] to get the eigenstates of elctron (hole) as the first step.

Considering the character of model potentials $U_i$ and the solvability of basis Hamiltonian, we, respectively, introduce effective infinite two-dimensional lateral parabolic confinement potential $U_{\rho i}^{\text{eff}}$

$$U_{\rho i}^{\text{eff}} = \alpha_i \rho_i^2 \tag{5}$$

and effective square well $U_{zi}^{\text{eff}}$ in $z$ direction

$$U_{zi}^{\text{eff}} = \begin{cases} \beta_i & \text{if } |z_i| > \dfrac{H}{2} \\ 0 & \text{if } |z_i| \leq \dfrac{H}{2} \end{cases} \tag{6}$$

to reflect the spatial confinement provided by $U_i$. Then, single particle $\hat{H}_i$ can be recomposed as

$$\begin{aligned} \hat{H}_i &= \hat{H}_{i0}(\alpha_i, \beta_i) + \hat{H}_i'(\alpha_i, \beta_i) \\ &= \frac{P_{\rho i}^2}{2m_i^*} + U_{\rho i}^{\text{eff}} + \frac{P_{zi}^2}{2m_i^*} + U_{zi}^{\text{eff}} + \hat{H}_i'(\alpha_i, \beta_i), \end{aligned}$$

where $\hat{H}_i' \equiv U_i - U_{\rho i}^{\text{eff}} - U_{zi}^{\text{eff}}$. The eigenenergies $(E_{ik}^{(0)})$ and corresponding eigenfunctions $\Phi_{ik}^{(0)}$ of $\hat{H}_{i0}(\alpha_i, \beta_i)$ can be solved analytically. The eigenfunctions $\Phi_{ik}^{(0)}$ can be written as

$$\Phi_{ik}^{(0)} = \Psi_{\vec{\rho}i}^{n_i, m_i}(\alpha_i; \vec{\rho}_i) \Psi_{zi}^{n_i^z}(\beta_i; z_i), \tag{7}$$

where $k = \{n_i, m_i, n_i^z\}$ generally indexes the basis.

Using $\Phi_{ik}^{(0)}$ as basis, the energy levels and wave functions of electron (hole) can be obtained by a VD process, which can be written as

$$\begin{cases} \displaystyle\sum_{k'} [(E_{ik}^{(0)} - E_{ij}) \delta_{k,k'} + \mathcal{H}_{i,k,k'}'] A_{ik'}^j = 0 \\ E_{ig} = \displaystyle\min_{\{\alpha_i, \beta_i\}} E_{i0} \end{cases}, \tag{8}$$

where we have defined $\mathcal{H}_{i,k,k'}' = \langle \Phi_{ik}^{(0)} | H_i' | \Phi_{ik'}^{(0)} \rangle$ and $A_{ik'}^j$ is the expansion coefficient of the eigenfunction. The detailed description of Newton's method in searching the minimum is as follows: 1. Initializing the parameters $\{\alpha_i, \beta_i\}$; 2. Solving $\{E_{ik}^{(0)}, \Phi_{ik}^{(0)}\}$; 3. Diagonalizing Hamiltonian matrix

$$\sum_{k'} [(E_{ik}^{(0)} - E_{ij}) \delta_{k,k'} + \mathcal{H}_{i,k,k'}'] A_{ik'}^j = 0,$$

4. Calculating the gradient of $E_{i0}$, adjusting the parameters and jumping to step 2 until the gradient reaches zero;

and 5. Finally getting the ground-state energy

$$E_{ig} = \min_{\{\alpha_i,\beta_i\}} E_{i0}.$$

Once the minimum of $E_{i0}$ is found, the ground and excited states of the QD can be obtained.

### C. Exciton states

It becomes more difficult for the calculation of incompletely confined exciton states because the attractive Coulomb interaction must be included. A set of appropriate basis including both effects of dot confinement and Coulomb interaction should be established to obtain energy spectra of exciton states with satisfied convergence. Such a basis, however, is difficult to be determined just by experience. The VD method is still the efficient way in such case.

To solve exciton Hamiltonian (1), we still employ the effective confinement potentials in Eqs. (5) and (6), and separate it into $z$ part and in-plane part, which is further separated into center-of-mass (CM) and relative parts with polar coordinates as

$$\begin{aligned}\hat{H}_{ex} &= \hat{H}_0 + \hat{H}' \\ &= \hat{H}_{\vec{\rho}}^{\mathrm{CM}}(\alpha_i) + \hat{H}_{\vec{\rho}}^{\mathrm{rel}}(\alpha_i,\lambda) + \sum_{i=e,h} \hat{H}_{zi}(\beta_i) + \hat{H}'(\alpha_i,\beta_i,\lambda)\end{aligned} \tag{9}$$

with

$$\hat{H}_{\vec{\rho}}^{\mathrm{CM}}(\alpha_e,\alpha_h) = \frac{P_{\vec{\rho}_{\mathrm{CM}}}^2}{2M} + (\alpha_e+\alpha_h)\rho_{\mathrm{CN}}^2, \tag{10}$$

$$\hat{H}_{\vec{\rho}}^{\mathrm{rel}}(\alpha_e,\alpha_h,\lambda) = \frac{P_{\vec{\rho}_{\mathrm{rel}}}^2}{2\mu} + \frac{\alpha_e m_h^2 + \alpha_h m_e^2}{M^2}\rho_{\mathrm{rel}}^2 - \frac{\lambda e^2}{\epsilon\rho_{\mathrm{rel}}}. \tag{11}$$

Here, to avoid the well-known poor convergence caused by Coulomb interaction under weak confinements, an effective Coulomb term with variational parameter $\lambda$ is introduced in relative in-plane part. Not for this, the solution for incompletely confined excitons is even impossible. $\hat{H}_{z_e}$, $\hat{H}_{z_h}$, and $\hat{H}_{\vec{\rho}}^{\mathrm{CM}}$ are analytically solvable. $H_{\vec{\rho}}^{\mathrm{rel}}$ can be solved exactly using the series-expansion method.[21] Thus, eigenvalues and eigenfunctions of $\hat{H}_0$ can be given as

$$E_k^{(0)} = E_{N,M}^{(0)}(\alpha_e,\alpha_h) + E_{n,m}^{(0)}(\alpha_e,\alpha_h,\lambda) + E_{n_e}^{(0)}(\beta_e) + E_{n_h}^{(0)}(\beta_h) \tag{12}$$

and

$$\Phi_k^{(0)} = \Psi_{\vec{\rho}_{\mathrm{cm}}}^{N,M}(\alpha_e,\alpha_h;\vec{\rho}_{\mathrm{cm}})\Psi_{\vec{\rho}_{\mathrm{rel}}}^{n,m}(\alpha_e,\alpha_h,\lambda;\vec{\rho}_{\mathrm{rel}}),$$

$$\Psi_{ze}^{n_e^z}(\beta_e;z_e)\Psi_{zh}^{n_h^z}(\beta_h;z_h), \tag{13}$$

where $(E_{n_e}^{(0)}, \Psi_{ze}^{n_e^z})$, $(E_{n_h}^{(0)}, \Psi_{zh}^{n_h^z})$, $(E_{N,M}^{(0)}, \Psi_{\vec{\rho}_{\mathrm{cm}}}^{N,M})$, and $(E_{n,m}^{(0)}, \Psi_{\vec{\rho}_{\mathrm{rel}}}^{n,m})$ are eigenvalues and eigenfunctions of $\hat{H}_{z_e}$, $\hat{H}_{z_h}$, $\hat{H}_{\vec{\rho}}^{\mathrm{cm}}$ and $H_{\vec{\rho}}^{\mathrm{rel}}$, respectively. Again, $k$ generally represents $\{N,M,n,m,n_e^z,n_h^z\}$. Taking $\Phi_k^{(0)}$ as basis, energy levels and wave functions of an exciton can be obtained with good convergence through exactly diagonalization. The proper set of variational parameters $(\alpha_e,\beta_e,\alpha_h,\beta_h,\lambda)$ can be determined by searching the minimum of ground-state energy as described in Sec. B.

From above results, the binding energy $E_b$ of the ground state of the excition can be calculated as

$$E_b = E_{e0} + E_{h0} - E_{ex}, \tag{14}$$

where $E_{e0}$, $E_{h0}$ and $E_{ex}$ denote the energies of the ground state of electron, hole, and exciton, respectively.

From the eigenstates of excitons, their oscillator strengths can also be obtained. Within dipole approximation, the polarization field of exciton is determined by matrix elements between exciton states and the vacuum state

$$\mu_{j0} = \langle 0|p\,\delta(\vec{r}_{\mathrm{rel}})|\Phi_j\rangle \propto \sqrt{2}p_{\mathrm{cv}}\Phi_j(\vec{R}_{\mathrm{CM}},\vec{r}_{\mathrm{rel}}=0), \tag{15}$$

where $p$ is the transition operator and $p_{\mathrm{cv}}$ is the element between the conductance and valence bands. Thus, the polarization field corresponds to wave function with respect to CM coordinate $\vec{R}_{\mathrm{CM}}$ as relative coordinate $\vec{r}_{\mathrm{rel}}=0$. Oscillation strength is proportional to the norm of integral of polarization field:[22–24]

$$F_j \propto \left| \int d\vec{\rho}_{\mathrm{CM}} d\vec{\rho}_{\mathrm{rel}} dz_e dz_h \Phi_j(\vec{\rho}_{\mathrm{CM}},\vec{\rho}_{\mathrm{rel}},z_e,z_h) \times \delta(\vec{\rho}_{\mathrm{rel}})\,\delta(z_e - z_h) \right|^2. \tag{16}$$

Besides these, the full width at half maximum (FWHM) of the norm of polarization fields of exciton ground states can be also obtained to indicate the luminescence area.

## III. RESULTS AND DISCUSSIONS

In the studies of GaN/$Al_xGa_{1-x}N$ QDs with small $x$, the material parameters are taken as $\varepsilon_r=9.5$, $m_e^*=0.2m_e$, and $m_h^*=1.4m_e$.[18,19] The band gap of GaN is taken as 3.46 eV (Ref. 10) and the conduct and valence-band offsets are, respectively, given by $\Delta E_C(x)=0.6x+5.05x^2\pm 0.03x$ (eV) and $\Delta E_V(x)=0.45x+2.57x^2\pm 0.05x$ (eV).[25] In the calculations, energy and size are scaled by exciton Rydberg $R_{ex}^*=26.38$ meV and exciton Bohr Radius $a_B^*=2.87$ nm in bulk GaN material, respectively.

### A. Incompletely confined excitons

First, we would like to determine the incomplete confinement regime for excitons. A finite confinement potential is provided by the disklike QD, thus, just like the case for a finite spherical square well, there are critical sizes for carriers having bound states. Critical sizes can be given by performing single-particle calculations. We take the calculation for a GaN/$Al_{0.1}Ga_{0.9}N$ QD as an example. At a given height the dot radius must be bigger than certain value to have bound states or vice versa. So critical sizes are presented by two critical curves in the height-radius plane, as shown in Figs.

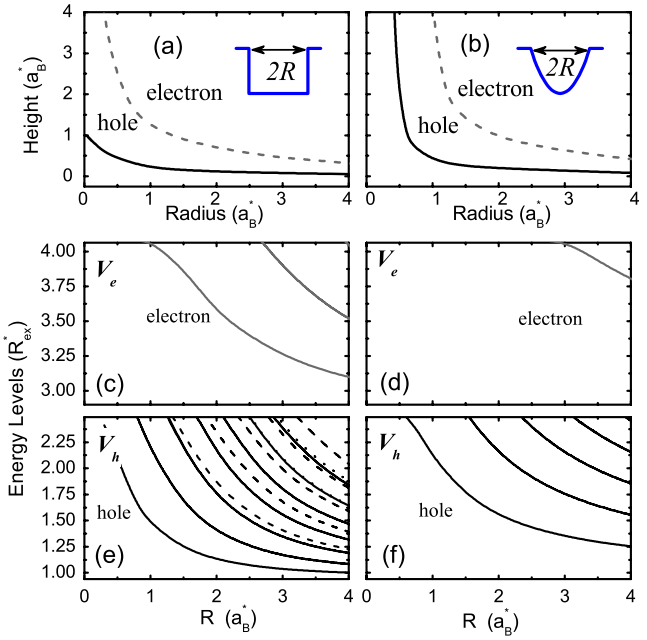


FIG. 1. (Color online) Critical curves for electrons and holes to have bound states in square confinement QD (a) and parabolic confinement QD (b) where insets depict the potential shapes. Variation of energy spectra along with radius for electrons and holes confined in square [(c) and (e)] and parabolic [(d) and (f)] confinement QDs with height $H=0.7a_B^*$.

1(a) and 1(b). Only at the right-up side of the upper curve can both carriers have bound states and we call it complete confinement regime. The area between two curves is the incomplete confinement regime, where only the hole is well confined in QD and the electron is localized by the hole through Coulomb attraction. Two types of confinement potential are adopted here as indicated by insets in Figs. 1(a) and 1(b) and similar behavior is shown. The only difference is that critical curves for square potential is lower than that for parabolic one, which means that the carriers in a parabolic confinement QD are more easily to escape as the dot gets smaller. In order to give a direct picture about effects of dot confinement on single carrier in QDs with different sizes, we plot in Figs. 1(c)–1(f) the dependence of energy levels on dot radius for both carriers confined in both types QDs with height $H=0.7a_B^*$. As radius decreases, ground-state energy increases tremendously, especially at small radius side. Compared to holes, electrons have less bound states and bigger energy differences between two levels.

Using VD method we can calculate the binding energy more precisely and efficiently. In Fig. 2, the evolution of binding energy with dot radius is shown for two types QDs. For relatively big radius, binding energy increases as dot radius deceases and approaches its maximum near the critical radius. Binding energy under parabolic confinement potential is larger than that under square one in complete confinement regime which indicates a stronger confinement. As the dot gets further smaller, it enters the incomplete confinement regime and, instead of being enhanced, the confinement is reduced by leakage of great portion of wave function into the matrix. Then the binding energy decreases rapidly toward

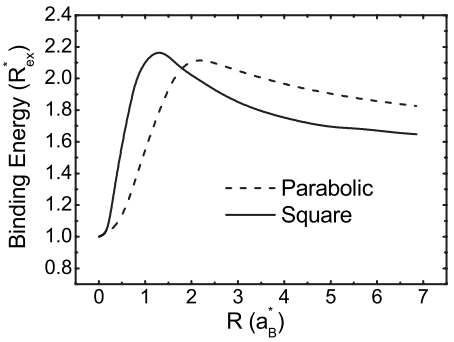


FIG. 2. Variation in binding energy along with dot radius for square (solid line) and parabolic (dashed line) confinement QDs with $H=0.7a_B^*$

$R_{ex}^*$, i.e., the binding energy of exciton in the bulk material. It is worthwhile to point out that the incomplete confinement effects have been also revealed in studying the shallow-deep transitions of impurities in semiconductor QDs.[26] What mentioned above means that the incomplete confinement effects of carriers widely exist in exciton and impurity states in QDs and can lead to interesting phenomena.

### B. Exciton spectra

The combined effect of spatial confinement and Coulomb interaction determines exciton states and makes it difficult for us to find a proper set of quantum indices to label exciton states. In VD method, however, this combined effect is included. As a result, components of exciton states are very concentrated, especially for ground states and low excited states. Therefore, we can label exciton states by their main components $(N,M;n,m;n_e^z,n_h^z)$, then we can study the evolution of energy levels along with dot size. We index the ground state with $a_0$ and several low-excited states with $a_i$, $b_0$, $b_i$, $c_0$, and $c_i$ $(i=1,2,\ldots)$. $a$ type states mainly contain the excitation of CM motion, for example, $a_0$, $a_1$, $a_2$, and $a_3$ are mainly (0,0;0,0;0,0), (1,0;0,0;0,0), (2,0;0,0;0,0), and (3,0;0,0;0,0), respectively. $b$ and $c$ types contain the intrinsic excitations of excitons. In particularly, $b_0$ is mainly radial excitation (0,0;1,0;0,0), and $c_0$ is mainly azimuthal excitation $(0,\pm 1;0,\mp 1;0,0)$.

By labeling and classifying exciton sates we can obtain a further understanding about the effect of dot confinement on energy spectra. Shown in Fig. 3 is the evolution of energy levels with dot radius for both square and parabolic confinement QDs. Number of bound states deceases rapidly as dot radius decreases. Energy levels of same type exciton states show similar behavior while those of different types cross each other, leading to changing in energy-level orders. Mainly composed by CM motion, $a$-type exciton states vary just like single-particle states as shown in Figs. 1(e) and 1(f). For $b$ and $c$ types, however, their energy-level orders become lower as radius deceases. This can be attributed to the competition between Coulomb interaction and dot confinement. In the regime of large radius, Coulomb interaction dominates relative motion and excitation of relative motion needs more energy than that of CM motion. As dot radius deceases, CM

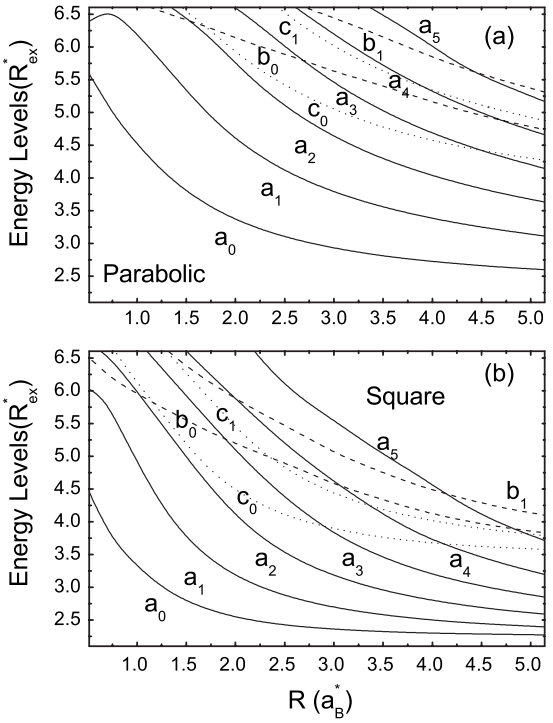


FIG. 3. Energy spectra of exciton confined in a parabolic confinement QD (a) and a square confinement QDs (b) with $H=0.7a_B^*$. The band gap $E_g$ has been extracted. Labels of energy level indicate their main component as discussed in the text.

excitation becomes more and more difficult. When it enters incomplete confinement regime, relative excitation replaces the role of CM excitation in low-excited states and the exciton becomes more hydrogenlike.

### C. Oscillator strengths

The coupling between the exciton and electromagnetic field is proportional to the oscillator strengths of the states. Then the studies of oscillator strengths modified by QD confinements are important for applications in quantum information and QDs coupled to microcavity. We plot in Figs. 4(a) and 4(b) the variation in oscillator strength with dot radius for both parabolic and square confinement QDs. For both potentials, the oscillator strengths of $a$-type exciton states increase almost linearly with increasing dot radius at relatively bigger radius. The differences within $a$-type exciton states in parabolic potential decrease while those in square-potential increase. In fact, under an infinite parabolic confinement oscillator strengths of $a$-type states are absolutely equal. Therefore oscillator strengths of $a$-type states in a parabolic confinement QD tend to approach each other as dot radius gets bigger and confining condition for them becomes more similar to that under infinite parabolic confinement. Under a square potential, however, $a$-type CM wave functions have almost the same distribution regime (in the whole dot), thus the more nodes (higher states) are, the less the value of integration is, and consequently, the weaker the oscillator strength is. Furthermore, the oscillator strength of $b_0$ is always weaker than that of $c_0$ for both types of potential

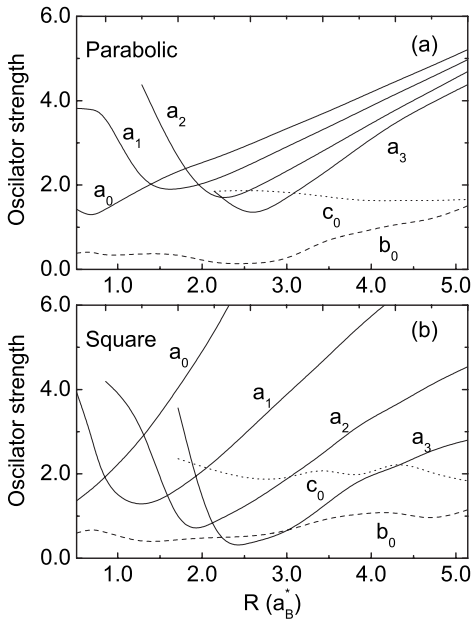


FIG. 4. Oscillator strengths of ground state and several low-energy excited states for parabolic (a) and square confinement and (b) QDs with $H=0.7a_B^*$. Labels here are same as those in Fig. 3.

since $b_0$ has more nodes in radial part of CM wave function than $c_0$.

The most interesting feature is the abnormal increase in oscillator strength of low $a$-type excited states in small dots. They can get even stronger than that of ground state. This is because small dot cannot provide good spatial confinement for these states and a great portion of CM wave function escapes into matrix, especially in incomplete confinement regime. Since $a_1$ or $a_2$ states extend much more broadly than $a_0$, their integrations are bigger than that of ground state, leading to their giant oscillator strengths.

### D. Polarization-field distribution

The luminescence area of an exciton is a main concern in optical experiments and applications of QDs. Although the spatial resolution of conventional optical devices is restricted to half the wavelength of the used light, current development in near-field optical-scanning microscopy technique enables us to overcome this limit.[27–29] In near-field optical experiments, the luminescence is mainly determined by single-exciton recombination, thus the luminescence area of QD can be simulated by the spatial distribution of polarization field of exciton ground state. Although the oscillator strength of the ground state does not change severely even in the incomplete confinement regime, the spatial distribution of polarization field can greatly depend on the size of the dot. In Fig. 5(a) we show dependences of the FWHM of the norm of polarization fields of exciton ground states on dot radius and height in $GaN/Al_{0.15}Ga_{0.85}N$ QDs. For the convenience in experiments, nanometer is used for the unit of length. It can be seen that for QDs with large sizes where the exciton is completely confined (typically $R>2.5$ nm and $H>1.5$ nm), the FWHM is mainly determined by the radius and very weakly depends on the height. The spatial distribution of

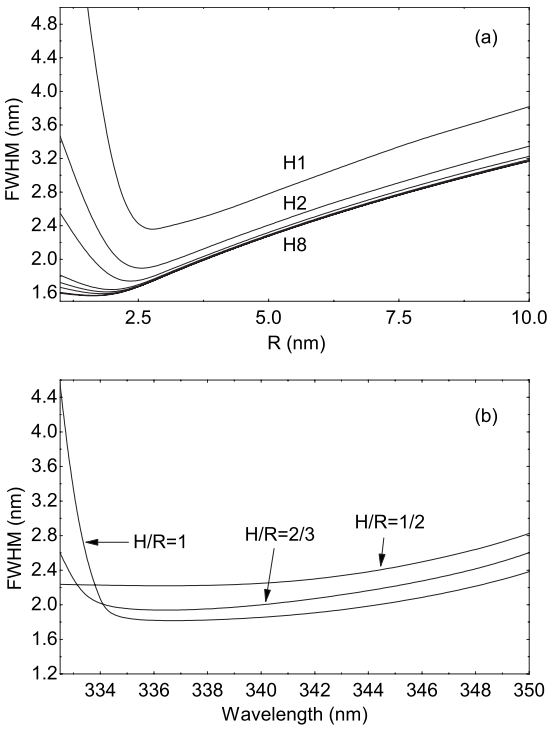


FIG. 5. (a) FWHM of norm of exciton-polarization fields as functions of $R$ in QDs with $H=1,2-8$ nm. (b) FWHM of exciton-polarization field as functions of emitted-photon wavelength in QDs with fixed height-to-radius ratio $H/R=1/2$, 2/3 and 1. Here $GaN/Al_{0.15}Ga_{0.85}N$ QDs are used.

polarization field is close to the confinement area of QDs, then the luminescence area will be proportional to the QD's area. On the contrary, for small QDs, the FWHM increases dramatically with the decrease in the radius and strongly depends on the height due to the incomplete confinement effects. Then there will be an abnormal relation between luminescence area and QD's size, which means that larger luminescence area may correspond to smaller QD size.

In some growth conditions, the QDs fabricated in experiments have fixed ratio between height and radius.[11] So we also plot the dependences of FWHM on height-to-radius ratio. And instead of the radius, the horizontal axis has been changed to emitted-photon wavelength which is usually given in experiments. In long-wavelength side, the FWHM decreases with the decrease of the wavelength. Again, the abnormal increase in FWHM is found in short-wavelength side where the exciton is incompletely confined. For $H/R=1$ the effect of incomplete confinement is more remarkable, as shown in Fig. 5(b). It is worthwhile to point out that an abnormal increasing in apparent size of GaN/AlN QDs at short-wavelength side is reported in a recent experiment.[30] In GaN/AlN QDs, the built-in electric field is strong which equivalently lowers confinement potentials for electrons and holes in $z$ direction, then the incomplete confinement effect may occur in QDs with larger sizes. We believe that the effect of incomplete confinement can also be observed in $GaN/Al_xGa_{1-x}N$ QDs with smaller sizes where the built-in electric field is weaker. And in recent experiment,[11] the sizes of $GaN/Al_xGa_{1-x}N$ QDs can indeed approach the critical size of incomplete confinement.

## IV. CONCLUSION

Noting the different optical behaviors between completely and incompletely confined excitons and using VD method, we have studied exciton states in $GaN/Al_xGa_{1-x}N$ QDs with small $x$. Combining the effects of confinement potential and Coulomb interaction, we can reasonably index the exciton states with their main excitation modes, which are quite different from those in QDs with infinite potentials.

As dot size becomes less than the critical size for electron but still larger than that for hole, incompletely confined exciton forms. Rather than being confined by the QD, electron is localized by the confined hole through attractive Coulomb interaction. Quantum behaviors of incompletely confined excitons are found quite different from those of completely confined ones. As dot size decreases, binding energy increases at first and achieves its maximum at about critical size, and then decreases rapidly. When the dot approaches the critical size, energy spectra become less dependent on potential shape and only a few levels exist below the band edge.

In incomplete confinement regime, the unusual enhancements in oscillator strengths of low-lying excited states and the FWHM of norm of ground-state polarization field are clearly shown. The incomplete confinement effect can appear in exciton and impurity states and even in corresponding charged states in QDs with smaller size and lower barrier. The studies may be useful for understanding some unusual optical phenomena displayed in these systems and also helpful for applications of QDs in photoelectronic devices.

## ACKNOWLEDGMENTS

Financial support from NSF China (Grants No. 10774085 and No. 10774016), the "863" Programme of China (Grant No. 2006AA03Z0404), and the MOST Programme of China (Grant No. 2006CB0L0601) are gratefully acknowledged.

*zjl-dmp@tsinghua.edu.cn

[1] F. Rol, S. Founta, H. Mariette, B. Daudin, L. S. Dang, J. Bleuse, D. Peyrade, J.-M. Gérard, and B. Gayral, Phys. Rev. B **75**, 125306 (2007).

[2] A. F. Jarjour, R. A. Oliver, A. Tahraoui, M. J. Kappers, C. J. Humphreys, and R. A. Taylor, Phys. Rev. Lett. **99**, 197403 (2007).

[3] A. Muller, W. Fang, J. Lawall, and G. S. Solomon, Phys. Rev. Lett. **101**, 027401 (2008).

[4] Y. Arakawa and H. Sakaki, Appl. Phys. Lett. **40**, 939 (1982).

[5] J. Stangl, V. Holy, and G. Bauer, Rev. Mod. Phys. **76**, 725 (2004).

[6] Y. Sugimoto, T. Saiki, and S. Nomura, Appl. Phys. Lett. **93**, 083116 (2008).
[7] J.-L. Zhu, S. F. Zhu, Z. Q. Zhu, Y. Kawazoe, and T. Yao, J. Phys.: Condens. Matter **10**, L583 (1998).
[8] S. Adachi, J. Appl. Phys. **58**, R1 (1985).
[9] M. Leszczynski, H. Teisseyre, T. Suski, I. Grzegory, M. Bockowski, J. Jun, S. Porowski, K. Pakula, J. M. Baranowski, C. T. Foxon, and T. S. Cheng, Appl. Phys. Lett. **69**, 73 (1996).
[10] S. C. Jain, M. Willander, J. Narayan, and R. Van Overstraeten, J. Appl. Phys. **87**, 965 (2000), and references therein.
[11] P. Ramvall, P. Riblet, S. Nomura, Y. Aoyagi, and S. Tanaka, J. Appl. Phys. **87**, 3883 (2000).
[12] S. De Rinaldis, I. D'Amico, E. Biolatti, R. Rinaldi, R. Cingolani, and F. Rossi, Phys. Rev. B **65**, 081309(R) (2002).
[13] C. Adelmann, B. Daudin, R. A. Oliver, G. A. D. Briggs, and R. E. Rudd, Phys. Rev. B **70**, 125427 (2004).
[14] V. Ranjan, G. Allan, C. Priester, and C. Delerue, Phys. Rev. B **68**, 115305 (2003).
[15] H. T. Jiang and J. Singh, Appl. Phys. Lett. **75**, 1932 (1999).
[16] T. Nakaoka, S. Kako, and Y. Arakawa, Phys Rev B **73**, 121305(R) (2006).
[17] J.-L. Zhu, W. D. Chu, Z. S. Dai, and D. Xu, Phys. Rev. B **72**, 165346 (2005).
[18] V. A. Fonoberov and A. A. Balandin, J. Appl. Phys. **94**, 7178 (2003).
[19] A. D. Andreev and E. P. O'Reilly, Phys. Rev. B **62**, 15851 (2000).
[20] A. D. Yoffe, Adv. Phys. **50**, 1 (2001).
[21] J.-L. Zhu, J. J. Xiong, and B.-L. Gu, Phys. Rev. B **41**, 6001 (1990); J.-L. Zhu, Z. Q. Li, J. Z. Yu, K. Ohno, and Y. Kawazoe, *ibid.* **55**, 15819 (1997).
[22] W. Que, Phys. Rev. B **45**, 11036 (1992).
[23] J. Song and S. E. Ulloa, Phys. Rev. B **52**, 9015 (1995).
[24] G. W. Bryant, Phys. Rev. B **37**, 8763 (1988).
[25] D. R. Hang, C. H. Chen, Y. F. Chen, H. X. Jiang, and J. Y. Lin, J. Appl. Phys. **90**, 1887 (2001).
[26] V. Ranjan and V. A. Singh, J. Appl. Phys. **89**, 6415 (2001).
[27] B. Hecht, B. Sick, U. P. Wild, V. Deckert, R. Zenobi, O. J. F. Martin, and D. W. Pohl, J. Chem. Phys. **112**, 7761 (2000).
[28] J. R. Guest, T. H. Stievater, G. Chen, E. A. Tabak, B. G. Orr, D. G. Steel, D. Gammon, and D. S. Katzer, Science **293**, 2224 (2001).
[29] K. Matsuda, T. Saiki, S. Nomura, M. Mihara, Y. Aoyagi, S. Nair, and T. Takagahara, Phys. Rev. Lett. **91**, 177401 (2003).
[30] Y. Z. Yao, T. Sekiguchi, Y. Sakunia, M. Miyamura, and Y. Arakawa, Scr. Mater. **55**, 679 (2006).